

This is the accepted version of the publication. This article may be downloaded for personal use only. Any other use requires prior permission of the author and AIP Publishing. This article appeared in Ng, C.-H., Chan, C.-W., Man, H.-C., Waugh, D., & Lawrence, J. (2016). Modifications of surface properties of beta Ti by laser gas diffusion nitriding. *Journal of Laser Applications*, 28(2), 022505 and may be found at <https://doi.org/10.2351/1.4944000>.

MODIFICATIONS OF SURFACE PROPERTIES OF BETA TI BY LASER SURFACE TREATMENT

Paper 203

Chi-Ho Ng^{1,3}, Chi-Wai Chan², Hau-Chung Man³, David Waugh¹, Jonathan Lawrence¹

¹ Laser Engineering and Manufacturing Research Centre, Faculty of Science and Engineering, University of Chester, Parkgate Road, Chester, CH1 4BJ, UK

² School of Mechanical and Aerospace Engineering, Queen's University, Belfast, BT9 5AH, UK

³ Department of Industrial and Systems Engineering, The Hong Kong Polytechnic University, Hong Kong, China

Abstract

β -type Ti-alloy is a promising biomedical implant material as it has a low Young's modulus but is also known to have inferior surface hardness. Various surface treatments can be applied to enhance the surface hardness. Physical vapour deposition (PVD) and chemical vapour deposition (CVD) are two examples of this but these techniques have limitations such as poor interfacial adhesion and high distortion. Laser surface treatment is a relatively new surface modification method to enhance the surface hardness but its application is still not accepted by the industry. The major problem of this process involves surface melting which results in higher surface roughness after the laser surface treatment. This paper will report the results achieved by a 100 W CW fiber laser for laser surface treatment without the surface being melted. Laser processing parameters were carefully selected so that the surface could be treated without surface melting and thus the surface finish of the component could be maintained. The surface and microstructural characteristics of the treated samples were examined using X-ray diffractometry (XRD), optical microscopy (OM), 3-D surface profile & contact angle measurements and nano-indentation test.

1. Introduction

Titanium (Ti) alloys, complementary to the conventional stainless steels and Co-Cr alloys, constitute one of the most important groups of materials for bio-implant applications. They possess the following desirable properties: high specific strength and modulus, good mechanical properties, as well as excellent biocompatibility and corrosion resistance [1-3]. Recent development on titanium alloys for bio-implant applications has been concentrated on the non-toxic and low modulus β titanium alloys (hereafter β -Ti). Several new groups of β -Ti made of non-toxic alloying elements such as Nb, Ta and Zr have been developed [4-6]. Among which, the Ti-Nb

based alloy is considered to be the most important [6]. Low young modulus offer the advantages to reduce the "stress shielding" effect, preventing the bone loss as the modulus is close to that of bone [4,8], whilst the non-toxic or non-allergic elements can minimize the possibility of developing negative side effects on the patient.

However, the nature of inferior wear behaviour and poor surface hardness of β -Ti will lineally reduce the service life of implants, especially for orthopaedic implants. Surface treatment is therefore needed to improve the surface hardness as well as tribological properties of β -Ti. The concept behind is to reinforce the surface with hard ceramic precipitates/phases, such as titanium nitride (TiN), which exhibits several desirable properties such as high hardness and wear resistance, good chemical stability and good physical stability [9]. This ceramic coating is widely used in manufacturing industry due to these enhanced properties. Such hard surface coating can be simply fabricated by chemical vapour deposition (CVD), physical vapour deposition (PVD), ion-beam deposition and radio-frequency (RF) magnetron sputtering [8-10]. However, in most of these methods, the substrate is need to be heated at elevated temperatures (range of 400–1000 °C), which may deteriorate its mechanical properties. In the current study, laser technology is used for surface-treating the Ti-Nb based alloy, giving rise to small changes in substrate temperature. Short treatment time and controllable accuracy of treatment location are the extra advantages of laser surface treatment. To this end, laser surface treatment is said to be an attractive alternative method compared to other surface treatment procedures.

This study successfully found out an optimal set of laser processing parameters to treat the Ti-Nb based material without surface melting. A compact and smooth surface was formed without significant surface roughening. The following findings such as surface microstructure characterization, 3-D

surface profile & contact angle measurements as well as nano-indentation test of the laser treated and untreated β -Ti alloys are reported and discussed in detail hereafter.

2. Experimental Methods

2.1 Materials

The material used in the study was Ti-35Nb based alloy. The samples of dimensions 15 mm x 10 mm x 3 mm were spark cut from original plates. The chemical composition of Ti-35Nb based alloy is depicted in Table 1. Before laser surface treatment, the surface of the samples was polished sequentially with a series of SiC papers down to 800 grits to remove any oxide layer. Subsequently the samples were cleaned and degreased ultrasonically in methanol bath for 10 min, rinsed in distilled water, and dried thoroughly in cold air stream prior to laser surface treatment.

Table 1. Chemical Composition of Ti-Nb base alloy (wt%).

Elements	Composition (wt%)
Ti	51.7
Nb	35.3
Zr	7.3
Ta	5.7
Ca	0.0023
Mg	0.0015
Fe	0.027
Mn	0.0018
Si	0.002
Zn	0.0006

2.2 Laser Surface Treatment

The laser surface treatment process was performed using a 100 W CW fiber laser (SPI Lasers, U.K.) with a wavelength of 1091 nm. The samples were positioned in a specifically-designed chamber which was continuously purged with pure nitrogen gas at a rate of 30 L/min to create a nitrogen zone during laser treatment. The samples were irradiated with a CW fiber laser using the following optimal processing parameters: laser spot (defocused) diameter = 1.1 mm, laser scanning speed = 1 mm/s, the overlap neighbouring tracks was 0.3 mm for constructing a continuous surface layer, laser fluence = 14.8 J/mm² (non-melted). These parameters were

carefully chosen after preliminary selection which gave rise to a reasonable uniform non-melted surface.

2.3 Characterization Methods

Optical microscopy (OM, Leica DM4000M, Germany) was used for preliminary observation of the surface morphology of the laser-treated samples. The phases present in the treated and untreated samples were identified using X-ray diffraction (XRD, Rigaku SmartLab, Japan) at 40 kV and 40 mA using CuK α radiation. In terms of surface roughness R_a , the 3-D surface profile and surface roughness of the laser treated and untreated samples were examined by optical measurement system (Wyko NT 8000, Veeco Instruments, Tucson, AZ, USA). Nano-indentation tests employing a diamond Berkovich indenter (Hysitron nano-mechanical test instrument, USA) were performed on untreated and treated samples. 4000 μ N was selected as the nano-indentation load, and the corresponding indentation depth for the treated sample was around 120 nm. Loading and unloading curves were acquired and the hardness H_N and reduced Young's modulus E_r were determined from the curves.

2.4 Contact Angle Measurement

To study the wetting properties of laser treated and untreated surfaces, the contact angle θ was determined by a goniometer (contact angle goniometer OCA 20 DataPhysics, Germany) implementing sessile drop method equipped with a CCD video camera. The samples were ultrasonically cleaned in an ethanol bath for 5 minutes and dried thoroughly in a cool air stream between measurements. Distilled water was used to measure the contact angle of each surface. 5 μ l droplet of each media was delivered from the tip of a micro-litre syringe. The images were captured by camera and the contact angle was acquired with computer software. For each sample 10 data points were performed for the laser treated and untreated surfaces and each experiment was conducted at room temperature. The mean value and standard deviation were then calculated from the experimental data. The surface energy was determined using the equation of state method implementing one liquid (water).

3. Results and Discussion

3.1 Surface Image Analysis

By careful selection of the laser processing parameters, a laser treated surface without melting was achieved. Figure 1 shows the laser-treated (non-melted) surface by overlapping neighbouring laser tracks. The surface of treated sample showed a golden-yellowish colour which likely indicates the formation of TiN on the surface of alloy [11].

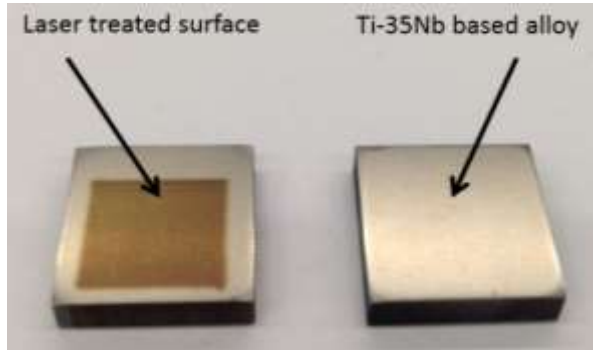


Figure 1. Images of the laser treated and untreated sample surface

3.2 XRD Analysis

X-ray diffraction (XRD) patterns corresponding to the laser treated and untreated surface are shown in Figure 2. The peaks in the diffraction pattern of bcc β phases are observed from both laser treated and untreated alloys. The untreated alloy exhibited only bcc β phases with highest intensity at β (110) peak. This is attributed to the large amounts of β stabilizing alloying elements (Nb, Zr & Ta) in Ti-Nb base alloy. Comparing to the untreated, the β (110) and β (200) peaks were diminished in the material after laser-treatment. It indicates that β phase might be reduced attributed to the formation of TiN. Nitrogen is known as a α stabilizer and TiN has an fcc structure (α phase). The incoherency between the parent β phases and the newly formed TiN in the microstructure may be the reason for the reduction of intensity in the β phase peak. Apart from the existence of TiN formation [12], the golden-yellowish layer could be other types of ceramic nitride compounds, given the presence of other reactive metal elements in the material. As a result, further study in the surface characterization

is needed for deeply understanding the microstructure on the surface by the laser treatment.

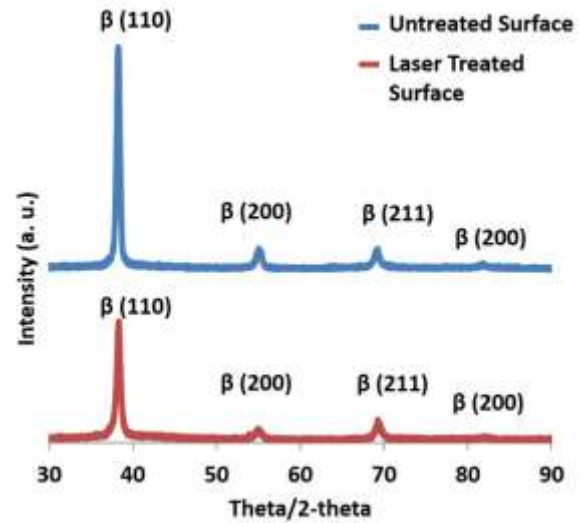


Figure 2. XRD patterns obtained from laser treated and untreated samples

3.3 Nano-Indentation Measurement

Continuously applying a small load of capability for nano-indentation can be commonly used for determination of the mechanical properties of thin layer, and the substrate effect can be reduced by a smaller resulting indentation depth [13]. A smooth load-displacement curve was obtained by the optimal selection of the loading and the acceptable indentation depth as shown in Figure 3. The hardness H_N , reduced Young's modulus E_r and H^3/E^2 ratio of treated and untreated samples are given in Table 2. The plastic deformation resistance (H^3/E^2 ratio) is an indicator of a resistance to plastic deformation of the coating and a relationship between the hardness H_N and the reduced Young's modulus E_r [14-15]. The wear resistance relates to the high hardness H_N and the reduced Young's modulus E_r [16]. Therefore, the plastic deformation can be minimized in the materials according to the high hardness H_N and low reduced Young's modulus E_r [17]. The toughness and plastic deformation resistance increased significantly after the laser surface treatment, and the treated sample was about 4 times than that of untreated sample.

The mechanism to improve the surface hardness lies in the formation of very hard surface layer on the material. It has been extensively discussed in

the authors' previous paper [12] that Ti can react with N_2 to form the very hard ceramic TiN layer. The beta-Ti used in this study is Ti-based (more than 50 % in concentration). It is reasonably to speculate that the hardness increment came directly from the formation of TiN.

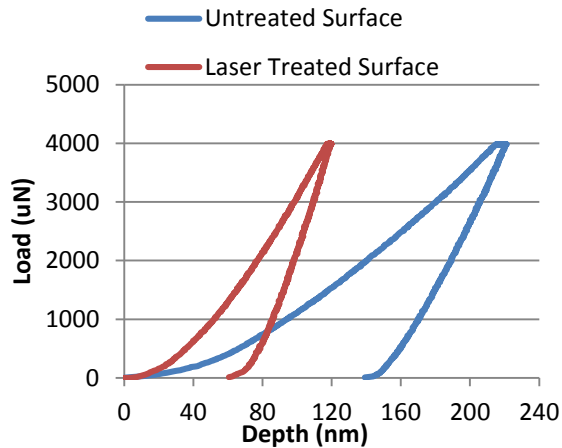


Figure 3. Nano-indentation curves of the treated and untreated samples

3.4 3-D Surface Profile Measurement

A typical 3-D surface profile depicting the surface roughness of both untreated and laser treated samples is shown in Figure 4. The R_a value of the untreated sample was 143 nm. In comparison, the R_a of the laser treated sample was slightly increased to 189 nm. Therefore, the surface roughness characteristic of the laser treated sample was similar to that of the untreated. This is in good agreement with the findings of a pervious study [12].

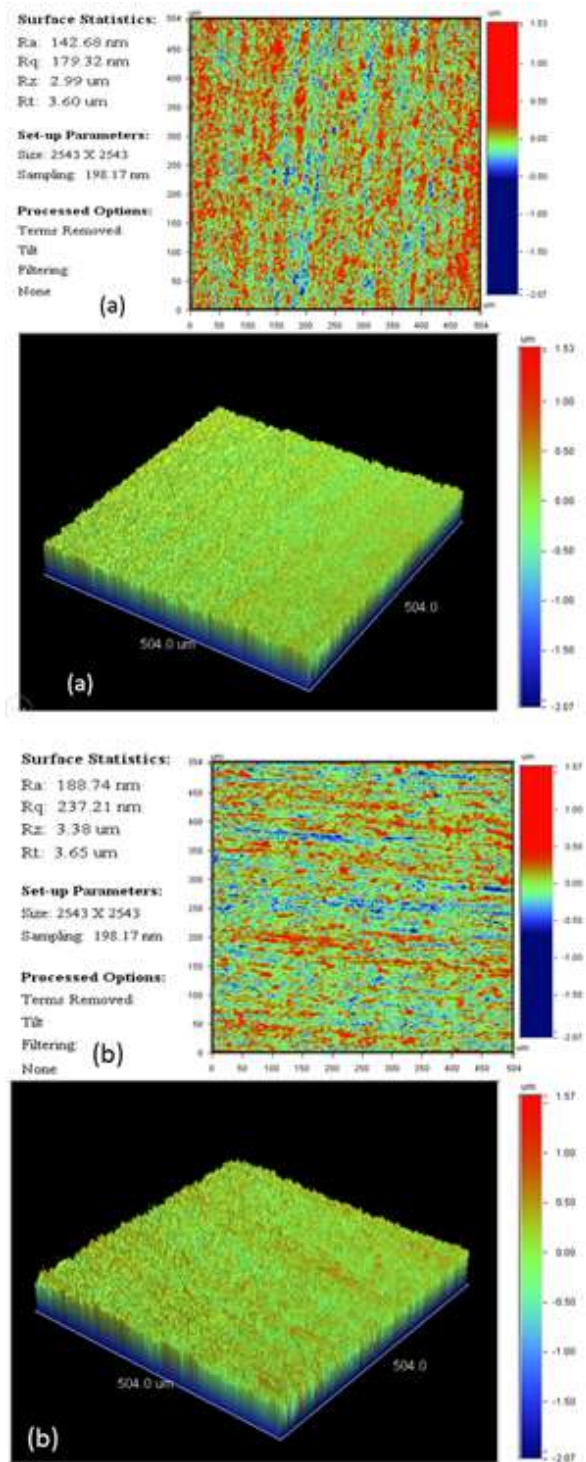


Figure 4. The 3-D profile and the measured surface roughness of (a) untreated and (b) laser treated samples

Table 2. Hardness H_N , reduced Young's modulus E_r and H^3/E^2 ratio of treated and untreated sample.

Properties	Untreated	Treated
Hardness H_N (GPa)	4.81	14.35
Reduced Young's modulus E_r (GPa)	63.87	171.24
H^3/E^2 ratio (GPa)	0.027	0.101

3.5 Contact Angle Measurement

To investigate the wetting properties of surface treated by laser, contact angle measurements were conducted for the laser treated and untreated sample using distilled water. The results are given in Table 3 and Figure 5. According to the American Society for Testing and Materials (ASTM) D7334-08 specifications [18], if the water contact angle is less than 45° the surface is hydrophilic surface, whereas the contact angle exceeds 90° the surface is hydrophobic. The laser treated and untreated samples exhibited a near hydrophilic nature. However, the untreated sample showed highest average contact angles of $66.16 \pm 4.14^\circ$ with distilled water. The surface energies of the laser treated and untreated surface 49.26 mN/m and 44.99 mN/m. From the above results, it can be observed that the laser surface treatment can enhance the hydrophilicity of the β -Ti surface, as evidenced by the decreased contact angles and increased surface energy. The current study is in good agreement with the literature that roughening the surface improves the wettability and therefore reduces the contact angle [19-20]. In addition, it has been reported [21] that TiN can improve the contact angle due to the increase of surface energy.

Table 3. Contact angles of the treated and untreated samples

Testing liquid	Untreated	Laser treated
Distilled water	$66.16 \pm 4.14^\circ$	$54.55 \pm 2.85^\circ$

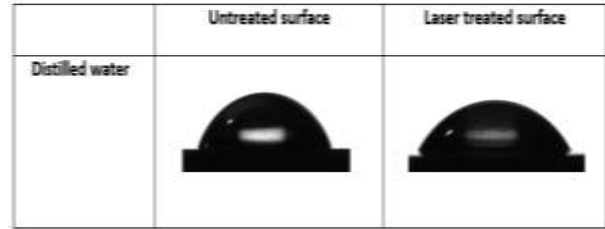


Figure 5. Images of contact angles of distilled water resting on the laser treated and untreated surface

4. Conclusions

Laser treatment on the Ti-Nb based alloy has been strived with an aim of acquiring the surface without melting. A comparative study of the surface characterization, wettability, surface roughness and nano-indentation of the laser treated and untreated samples have been compared. The following conclusions were reached:

1. With the laser fluence and nitrogen gas flow rate fixed at 14.8 J/mm^2 and 30 L/min , the optimal laser scanning speed and the laser beam diameter are 1 mm/s and 1.1 mm for achieving non-melt surface of treated sample;
2. The golden-yellowish ceramic layer on the laser-treated surface was likely to be TiN;
3. The average roughness of the laser treated and untreated sample were similar, which was slightly increased around 46 nm (surface roughness R_a) after laser surface treatment;
4. After the laser surface treatment, the sample surface hardness was increased by approximately 4 times;
5. Laser treated surfaces increased the hydrophilicity and increased surface energy giving rise to a lower contact angle.

Acknowledgement

The work described in this paper was supported by research grants (G-YK36 and G-YM75) from the Hong Kong Polytechnic University, Hong Kong Special Administration Region, China. The PhD studentship of Chi-Ho Ng is supported by the University of Chester, UK.

References

- [1] Prince, M.R. Salzman, E.W. Schoen, F.J. Palestrant, A.M. Simon, M. (1988) Local intravascular effects of the nitinol wire blood clot filter, *Invest. Radiol.* 23, 294-300.
- [2] Kasano, F. Morimitsu, T. (1997) Utilization of nickel-titanium shape memory alloy for stapes prosthesis. *Auris Nasus Larynx* 24, 137-142.
- [3] Ryhanen, J. Kallioinen, M. Serlo, W. Peramaki, P. Junila, J. Sandvik, P. Niemela, E. Tuukkanen, J. (1999) Bone healing and mineralization, implant corrosion, and trace metals after nickel-titanium shape memory metal intramedullary fixation. *Journal of Biomedical Materials Research* 47, 472-480
- [4] Yang, G. Zhang, T. (2005) Phase transformation and mechanical properties of the $Ti_{50}Zr_{30}Nb_{10}Ta_{10}$ alloy with low modulus and biocompatible, *Journal of Alloys and Compounds* 392, 291-294.
- [5] Geetha, M. Singh, A.K. Gogia, A.K. Asokamani, R. (2004) Effect of thermomechanical processing on evolution of various phases in Ti-Nb-Zr alloys, *Journal of Alloys and Compounds* 384, 131-144.
- [6] Long, M. Rack, H.J. (1998) Titanium alloys in total joint replacement – a materials science perspective, *Biomaterial* 19, 1621-1639
- [7] Zhou, Y.L. Niinomi, M. Akahori, T. Fukui, H. Toda, H. (2005) Corrosion resistance and biocompatibility of Ti-Ta alloys for biomedical applications, *Material and Science Engineering A* 398, 28-36.
- [8] Rudenja, S. Leygraf, C. Pan, J. Kulu, P. Taliments, E. Mikli, V. (1999) Duplex TiN coatings deposited by arc plating for increased corrosion resistance of stainless steel substrates, *Surface and Coatings Technology* 114 129.
- [9] Shimadaa, S. Takadaa, T.Y. Tsujino, J. (2005) Deposition of TiN films on various substrates from alkoxide solution by plasma-enhanced CVD, *Surface and Coatings Technology* 199, 72-76
- [10] Altun, H. Sinici, H. (2008) Corrosion behavior of magnesium alloys coated with TiN by cathodic arc deposition in NaCl and Na_2SO_4 solution, *Materials Characterization* 59, 266-270.
- [11] Weimer, A.W. (1997) Carbide, Nitride and Boride Materials Synthesis and Processing, first ed. Chapman & Hall, London,
- [12] Man, H.C. Bai, M. Cheng, F.T. (2011) Laser diffusion nitriding of Ti-6Al-4V for improving hardness and wear resistance, *Applied Surface Science* 258, 436-441
- [13] Tsui, T.Y. Vlassak, J. Nix, W.D. (1999) Indentation plastic displacement field: Part II. The case of hard films on soft substrates. *Journal of Materials Research* 14, 2204-2209
- [14] Caicedo, J.C. Zambrano, G. Aperador, W. Escobar-Alarcon, L. Camps, E. (2011) Mechanical and electrochemical characterization of vanadium nitride (VN) thin films, *Applied Surface Science* 258, 312-320.
- [15] Kim, G.S. Lee, S.Y. Hahn, J.H. Lee, S.Y. (2003) Synthesis of CrNyAlN superlattice coatings using closed-field unbalanced magnetron sputtering process, *Surface and Coatings Technology* 171, 91-95.
- [16] Leyland, A. Matthews, A. (2000) On the significance of the H/E ratio in wear control: a nanocomposite coating approach to optimised tribological behavior, *Wear* 246, 1-11.
- [17] Tsui, T.Y. Pharr, G.M. Oliver, W.C. Bhatia, C. S. White, R. L. Anders, S. Anders A. and Brown, I. G. (1995) Nanoindentation and nanoscratching of hard carbon coatings for magnetic disks, *Material Research Society Symposium Proceedings* 383 447.
- [18] American Society for Testing and Materials (ASTM) D7334-08, Standard Practice for Surface Wettability of Coatings, Substrates and Pigments by Advancing Contact Angle Measurement, ASTM International, West Conshohocken, PA, USA, 2013.
- [19] Mirhosseini, N. Crouse, P.L. Schmidh, M.J.J. Li, L. Garrod, D. (2007) Laser surface micro-texturing of Ti-6Al-4V substrates for improved cell integration, *Applied Surface Science* 235, 7738-7743
- [20] Jeong, Y.H. Son, I.B. Choe, H.C. (2011) Formation of surface roughness on the Ti-35Nb-xZr alloy using femtosecond laser for biocompatibility, *Procedia Engineering* 10, 2393-2398
- [21] Amadeh, A. Heshmati-Manesh, S. Labbe, J.C. Laimeche, A. Quintard, P. (2001) Wettability and corrosion of TiN, TiN-BN and TiN-AlN by liquid steel, *Journal of the European Ceramic Society* 21, 277-282